The multifocal electroretinogram (mfERG) and cone isolating stimuli: Variation in L- and M-cone driven signals across the retina

Johannes Albrecht Division of Experimental Ophthalmology, University Eye Hospital, Tübingen, Germany

Herbert Jägle Division of Experimental Ophthalmology, University Eye Hospital, Tübingen, Germany

Donald C. Hood Department of Psychology, Columbia University, New York, NY, USA

Lindsay T. Sharpe Department of Experimental Psychology, University of Newcastle, Newcastle-upon-Tyne, UK

Multifocal electroretinograms (mfERG) were recorded from 38 normal trichromats with a pattern-reversing display that modulated only their long-wavelength sensitive (L) or only their middle-wavelength sensitive (M) cones at equal cone contrasts and average quantal catches. The display consisted of scaled, 103 hexagonal elements, subtending 84° x 75° of visual angle. Typically, the amplitude of the L-cone driven signal was greater than that for the M-cone driven one at all retinal eccentricities, but large differences were found among observers. These values correlated with L- to M-cone ratios obtained psychophysically in the same observers using 2° (dia.) heterochromatic flicker photometry. Interestingly, the L- to M-cone driven amplitude ratios differed between the central and peripheral retina. For the central fovea (5° dia.), the mean ratio was 1.4 ± 0.6 (for the N1P1 component), whereas for the annular ring centered at 40° in the periphery, it was 2.3 ± 2.0. The mean P1 latency of the summed M-cone driven mfERG (28.0 ± 2.6 ms) was significantly advanced relative to the L-cone driven signal (29.0 ± 1.9 ms), but the mean N1 latencies were similar (15.6 ± 1.7 ms and 16.2 ± 1.3 ms, respectively). The P1 latency difference between the L- and M-cone driven waveforms was not found in the central 5° (dia.) of the retina. However, it increased with retinal eccentricity. The regional differences in the amplitudes and latencies of the L- and M-cone driven mfERG signals can be related to variations in the L- to M-cone ratios and/or the receptor to bipolar gain factors that depend on eccentricity.

Keywords: color vision, cones, retinal cone mosaic, electroretinography (ERG), multifocal electroretinography (mfERG)

Introduction

Recently, we have used a cone silent substitution technique, based on the Stockman and Sharpe (2000) cone fundamentals, to modulate only the long-wavelength sensitive (L) or only the middle-wavelength sensitive (M) cones in the human multifocal electroretinogram (mfERG). These procedures allow us to quantify topographical variations in the integrity of L- and M-cone driven mfERG signals in clinical patients. Here we exploit the cone isolating mfERG to obtain information about topographical variation in the processing of L- and M-cone driven signals across the retina in normal observers.

Current molecular genetic models of L- and M-cone photopigment gene expression are consistent with greater L- than M-cone photopigment gene expression (Nathans, Thomas, & Hogness, 1986; for a review, see Sharpe, Stockman, Jägle, Knau, & Nathans, 1999). This greater L- than M-cone photopigment expression was originally inferred from both psychophysical and electrophysiological studies, involving techniques as diverse as heterochromatic flicker photometry (HFP) (De Vries, 1946, 1948; Kremers et al., 2000), psychophysical detection thresholds (Cicerone & Nerger, 1989; Vimal, Pokorny, Smith, & Shevell, 1989; Pokorny, Smith, & Wesner, 1991; Wesner, Pokorny, Shevell, & Smith, 1991), Ganzfeld flicker electroretinography (Carroll, McMahon, Neitz, & Neitz, 2000; Kremers, et al., 2000), retinal densitometry (Kremers et al., 2000), and high resolution optical imaging (Roorda & Williams, 1999). The L- to M-cone ratios derived from such studies range from 0.3:1 to 8.7:1, depending on target location and size. However, these procedures provide either small local (usually central foveal) or large-field retinal estimates. By contrast, molecular biological analysis of opsin mRNA assayed from postmortem human eyes has provided topographical estimates (Hagstrom, Neitz, & Neitz, 1997, 1998), which suggest a central L- to M-cone ratio of 1.5:1

DOI 10:1167/2.8.2 Received July 30, 2001; published November 25, 2002 ISSN 1534-7362 © 2002 ARVO

with an increase to 3.0:1 in the mid-periphery (circa 41° eccentricity). But the resolution obtained with this technique so far does not allow conclusions to be made concerning the cone ratio in the central 10°.

The cone isolating mfERG offers advantages that nicely compensate for the resolution and regional limitations inherent to the psychophysical, ERG, and mRNA studies. With the mfERG technique, it is possible to isolate L- and M-cone driven signals with a resolution of about 5° (dia.) of visual angle over a large visual area (84° x 75°). However, the straightforward interpretation of mfERG amplitudes with regard to L- and M-cone distributions is complicated by the complexity of the mfERG waveform. It consists of two initial major components, which are analogues of the a- and b-waves of the full-field flash ERG (Hood, Seiple, Holopigian, & Greenstein, 1997): an initial negative deflection (N1) followed by a positive peak (P1). In addition, there is a second prominent negative deflection (N2) present as well.

Chemical isolation of components of both the full-field and mfERG of monkeys has established that the N1 component is largely an OFF-bipolar response with relatively small contributions from the inner retina and the cone photoreceptors (Sieving, Murayama, & Naarendorp, 1994; Horiguchi, Suzuki, Kondo, Tanikawa, & Miyake, 1998; Hare et al., 2001; Hood, 2000; Hood, Frishman, Saszik, & Viswanathan, 2002a). In contrast, the P1 component is predominantly produced by the onset of the ON-bipolar cells and to some extent by the offset of the OFF-bipolars, and the N2 component is largely produced by the offset of both the ON-bipolars and OFF-bipolars (Hood et al., 2002a). Obviously, any attempt to relate the ratio of L- to M-cone driven mfERGs to L- to M-cone photoreceptor mosaic ratios requires a comprehensive model of how these distal neural components alter the waveform. Nevertheless, a simplified model assuming a close relation between L- and M-cone driven mfERG amplitudes and L- to M-cone ratios may be justified, under limited conditions.

Here we present evidence to establish such a relation, including (1) comparisons of the L- and M-cone isolating response waveforms, (2) their amplitude versus intensity responses at five levels, (3) their contrast responses at two levels, and (4) correlations between the mfERG L- to M-cone estimates and estimates obtained in the same group of observers using a psychophysical HFP technique. The evidence, analysed topographically, is roughly consistent with the simplified model, although the model holds less well for the peripheral retina (> 5° of visual angle) than it does for the central fovea (< 5°). Additionally, the data provide insight into how regional differences in the amplitudes and latencies of the L- and M-cone driven mfERG signals can be related to variations in the L- to M-cone ratios and in gain factors in the outer retina. Finally, this work serves as a basis for interpreting evidence obtained from L- and M-cone isolating multifocal visually evoked potentials (mfVEPs), relying on the same cone isolating procedures that are presented in an accompanying study (Hood et al., 2002b).

Methods

Subjects

Thirty-eight trichromats, 25 males and 13 females (aged 19 to 51 years), participated in our study. All had normal (corrected) visual acuity and were classified as color normal on the basis of their performance on standard color vision tests, including the Ishihara pseudoisochromatic plates and the Nagel Type I anomaloscope. One of the normal trichromat females (J.B.) is a heterozygotic carrier for protanopia, as established by the family pedigree (the maternal grandfather is a protanope) and by preliminary molecular genetic analysis. In addition, 4 protanopes (aged 21 to 33 years) and 5 deuteranopes (aged 22 to 38 years) were tested. The classification of protanopia and deuteranopia was based on Rayleigh red-green equation matches made on the Nagel Type I anomaloscope (Schmidt & Haensch, Berlin, Germany). The genotypes of the dichromats were determined by molecular genetic (DNA) analysis of venous blood samples. There was no evidence of a functional M-cone opsin gene in the deuteranopes or of a functional L-cone opsin gene in the protanopes. In all subjects, one or both eyes were maximally dilated (circa 8 mm) by application of a mydriatic (0.5% tropicamide) and kept light-adapted before and during the mfERG recording. Corneal mfERG responses were measured with a DTL fiber electrode. The reference and ground skin electrodes were attached to ipsilateral temple and the forehead, respectively. Informed consent was obtained from all subjects after explanation of the purpose and possible consequences of the study. This study was conducted in accordance with the tenets of the Declaration of Helsinki and with the approval of the Institutional Ethics Committee in Human Experimentation at the University of Tübingen.

Visual Stimulation and mfERG Recording

The stimulus was generated on a flat-screen SONY Trinitron monitor with a resolution of 1024 x 768 pixels. It consisted of 103 hexagonal elements (see Figure 1), which subtended 84° x 75° of visual angle at a viewing distance of 18 cm. Each element was alternated in color pseudorandomly between two values carefully selected to modulate activity in a single cone class. The mfERG stimulation and data collection and analysis were performed by VERIS system software (Version 3.0.1) from EDI [see Sutter (1991) and Sutter & Tran (1992) for more details]. The appropriate colors or cone isolating stimuli were calculated from the emission spectra of the three phosphors and the Stockman and Sharpe cone

fundamentals, determined for 10° and larger viewing conditions (Stockman & Sharpe, 1998, 1999, 2000).

The emission spectra of the red, green, and blue phosphors of the monitor were measured with a compact array spectroradiometer (CAS 140, Instrument Systems, München, Germany). The calibration of the monitor was performed under the same conditions as the experiments. The red phosphor had its primary peak at 627 nm (full bandwidth at half-maximum [FBHM] = 4 nm) and a secondary peak at 707 nm (FBHM = 6 nm); the energy of which was 60% of that of the primary peak. The green phosphor had its peak at 522 nm (FBHM = 80 nm) and the blue at 453 nm (FBHM = 63 nm). The maximum intensities of the red, green, and blue phosphors were 24, 79.3, and 13.8 cd/m^2, respectively. Linearity tests established that the emission spectra of the three phosphors did not significantly change for the various luminance levels used during stimulation.

The modulation of cone excitation was quantified by the cone contrast formula

$$100\% \text{ x } (E_{max} - E_{min})/(E_{max} + E_{min}), \quad (1)$$

where E_{max} and E_{min} are, respectively, the maximal and minimal cone excitations. For our phosphor conditions, it was possible to obtain a maximum cone contrast of 47% for either the L- or the M-cone isolating stimuli, while maintaining the contrast of the remaining long-wavelength cone type (i.e., either L- or M-cones) and the S-cones at 0%. The rod system contribution to the mfERG was suppressed by the bright, rapidly alternating stimulus and by maintaining the ambient room luminance falling on the monitor screen at 150 cd/m^2.

The mean luminances of the L- and M-cone isolating stimuli were 19.2 cd/m^2 and 33.8 cd/m^2, respectively; corresponding to average quantal catches of approximately 4.46 log quanta·s^{-1}·cone^{-1} for the L-cones under the L-cone modulating condition and 4.43 log quanta·s^{-1}·cone^{-1} for the M-cones under the M-cone modulating condition (for details about the conversions, see Pugh, 1988, and Wyszecki & Stiles, 1982). Nearly identical cone contrast and average cone quantal catches for the L- and M-cones were chosen to ensure that both cone classes were stimulated at the same adapting level and to allow direct comparisons between the amplitudes and latencies of their mfERG signals.

The continuous mfERG recordings were amplified by 200 k with the low and high frequency set at 10 and 100 Hz for half amplitude (Grass Instruments) and were sampled at 1200 Hz. The frame rate was 75 Hz and the pseudo random m-sequence had 2^{14}-1 elements, corresponding to a total recording time of 3 min and 38.5 s for each condition. In total, 16,383 patterns were presented, in which each of the 103 hexagons changed pseudorandomly between two colors. To improve the subject's ability to maintain fixation, the experimental runs were broken up into 16 overlapping segments, each lasting 13.65 s. The L- and M-cone isolating recordings for each subject were obtained in a single session (with random assignment of order), under identical electrode placement and amplification conditions, to make the results comparable.

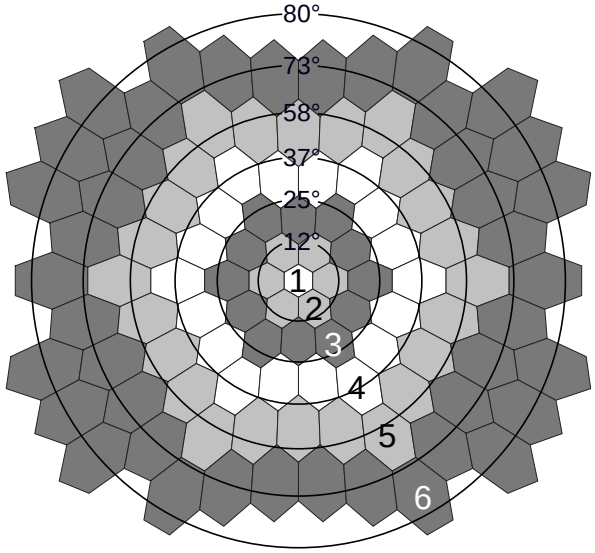

Figure 1. Schematic representation of the 103 independent hexagons employed in the mfERG paradigm. The numbers indicate the six concentric rings used to analyse the summed signals. Note that the size of the hexagons changes from center to periphery to compensate for the variation in cone density with retinal eccentricity and to ensure that the hexagons produce multifocal ERG responses of approximately equal amplitude (Sutter & Tran, 1992).

Results

Dichromat Data

To establish the reliability of the silent substitution method, we recorded the mfERG responses to the L- and M-cone modulation stimuli in color-blind observers who lack either the function of the L- (protanopes) or M- (deuteranopes) cones. Figure 2 displays their mfERG responses, summed over all 103 hexagons for the eye tested. As expected, the summed mfERG responses to L-cone modulation (Figure 2A) were absent or below the noise level in the four protanopes, and those to M-cone modulation (Figure 2D) were absent or below the noise level in the five deuteranopes. In contrast, the mfERG responses to pure modulation of the remaining M- or L-cone class were robust (Figure 2B and 2C). The absence of any signal for pure M-cone modulation in the deuteranopes (Figure 2D) is reassuring for it additionally establishes that under our photopic conditions the rods are not contributing to the mfERGs. It is important to prevent rod intrusion, especially for the M-cone isolating

stimulus, because of the similarity of the rod spectral sensitivity to that of the M-cones.

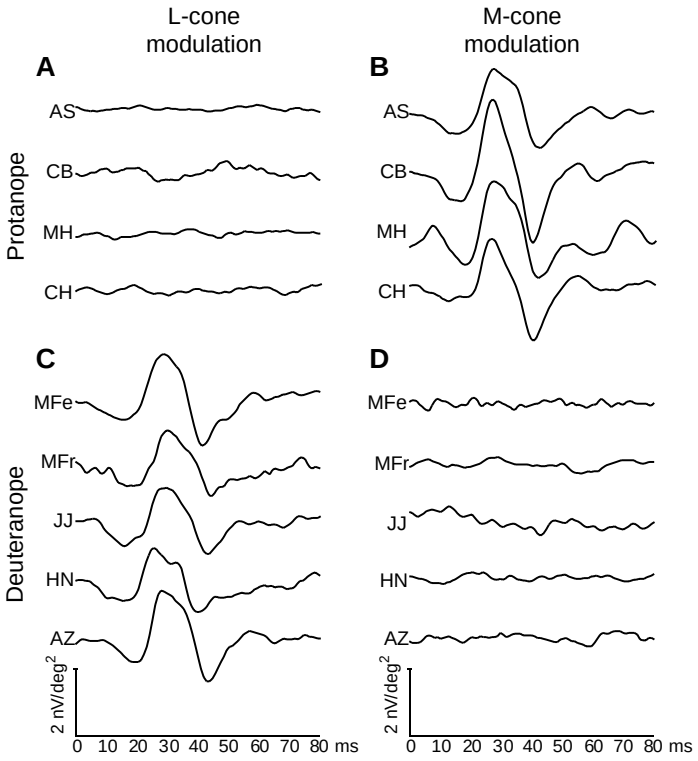

Figure 2. The mfERG responses (summed from all 103 hexagons and normalized) obtained from four protanopes (A & B) and five deuteranopes (C & D) for the L- (left column) and M- (right column) cone isolating stimuli. The inset at the bottom of the panels indicates the scale.

Intensity Response Series

To validate that the relative amplitudes of the L- and M-cone driven signals do not change with luminance level, we measured intensity response series, from 3.8 to 19.2 cd/m^2 for the L-cone driven signals and from 6.8 to 33.8 cd/m^2 for the M-cone driven signals, at a constant cone contrast of 47%. Figure 3 summarizes the results obtained for observer A.Y. (OD), a subject with nearly equal L- and M-cone driven responses (see Table 1). The traces have been summed for the L- (A, red curves) and M- (B, green curves) cone isolating conditions, and then further analysed in terms of amplitude (C) and latency (D), as a function of luminance, for both the N1 and N1P1 (the difference between the N1 minimum and the P1 maximum; see Figure 3 for the definitions of N1 and P1). (All latencies here and in subsequent figures are measured from the beginning of the trace to the peak of the component of interest.) Clearly, with increasing luminance, for both the L- and M-cone driven signals, the amplitude of both components increases in magnitude at a similar rate and there is a corresponding reduction in latency. Thus there is no significant change in the ratio of the L- to M-cone driven amplitudes of the mfERG over the range of luminances tested.

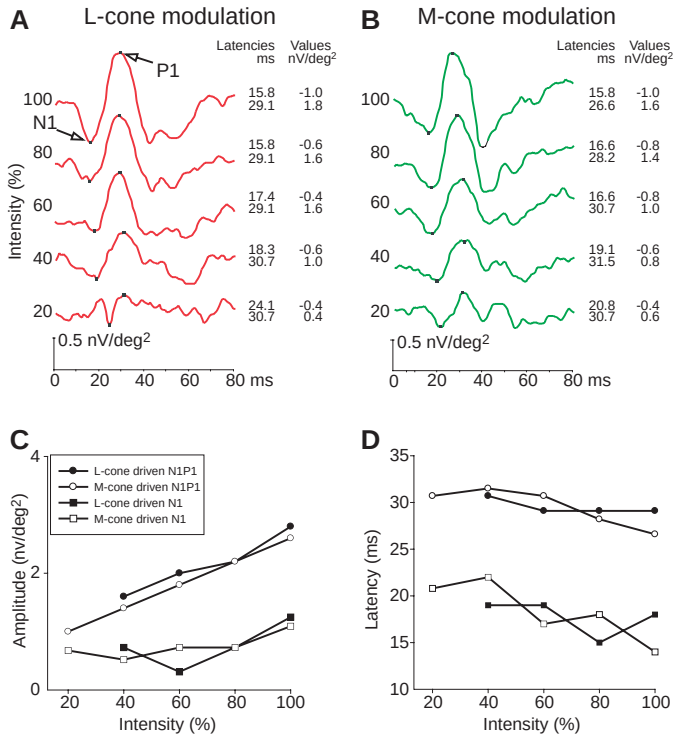

Figure 3. Intensity response series for the mfERG responses of one subject (A.Y.), with nearly equal L- and M-cone driven responses, obtained under the L- (Panel A, red curves) and M- (Panel B, green curves) cone isolating conditions. The intensity was increased from 3.8 to 19.2 cd/m^2 for the L-cones and from 6.8 to 33.8 cd/m^2 for the M-cones, at a constant cone contrast of 47%. The individual focal responses have been summed within the entire field depicted in Figure1. The latencies and amplitude values given at the right of the traces correspond to the two cursor positions (filled square). Panels C and D depict amplitude and latency responses as a function of increasing luminance, for both the N1 and P1 components of the mfERG, summed over the full field. N1 and P1 are labeled on the upper left trace.

Contrast Response Series

To establish that the relative amplitudes of the L- and M-cone driven signals are independent of contrast level, we measured the signals at two different contrasts, 27% and 47%. The luminance was held constant at 19.2 cd/m^2 for the L-cones and 33.8 cd/m^2 for the M-cones. Figure 4 summarizes the results obtained for two observers, for whom the responses from both eyes are shown: M.K. (see Table 1), who has an L-cone driven amplitude (red curves), which is a factor 2.4 greater than her M-cone driven amplitude (green curves), and E.L., who has more nearly equal L- and M-cone driven responses (factor 1.4). For the two observers, the calculated L- to M-cone driven ratios, averaged over both

eyes, are very similar at both contrasts: 2.37 ± 0.14 (M.K.) and 1.37 ± 0.14 (E.L.) for 27% contrast and 2.35 ± 0.07 (M.K.) and 1.25 ± 0.07 (E.L.) for 47% contrast. Thus, within the range of values tested, the L- and M-cone driven amplitudes appear to be linear with contrast, with the M- and L-cone driven responses both increasing, on average, by a factor of 1.5 for M.K. and 1.6 for E.L., going from 27% to 47% contrast.

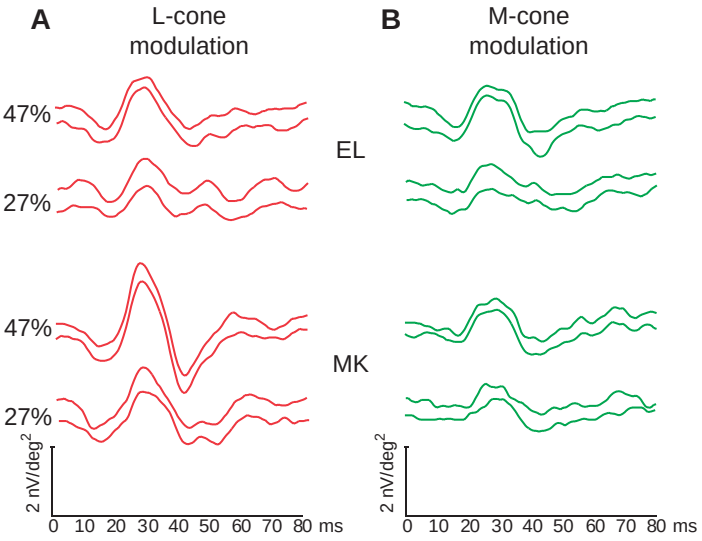

Figure 4. The L- (A, red curves) and M- (B, green curves) cone driven mfERG signals measured for two subjects under two contrast conditions, 47% (our standard condition) and 27% (a lower contrast condition). E.L. is a subject with nearly equal L- and M-cone driven responses; M.K. has an L-cone driven amplitude that is a factor 2.4 greater than her M-cone driven amplitude (see Table 1). The individual focal responses have been summed over the entire field depicted in Figure1 and the results have been averaged for the left (upper trace) and right (lower trace) eyes.

Full Field L- and M-Cone Driven Amplitudes

The data obtained for the maximum contrast level (47%) are summarized in Tables 1 and 2. These tables list the amplitudes and latencies of the N1 and P1 components of the mfERG responses, summed over all 103 hexagons, for each of the 38 observers. (Note the latencies are given for P1, but the amplitudes are given for N1P1: the difference between the minimum of the first negative peak [N1] and the maximum of the first positive peak [P1]). In 23 of the 38 subjects (10 females and 13 males), mfERGs were simultaneously recorded from both eyes.

The amplitude data (Table 1) indicate that the L-cone driven N1 and N1P1 signals are typically larger than the M-cone driven ones; the large inter-individual variability in amplitude notwithstanding. Averaged over all subjects, the mean L-cone driven signal amplitudes for the N1 and N1P1 components are 0.62 ± 0.30 nV/deg^2 and 1.65 ± 0.79 nV/deg^2, respectively, whereas the mean M-cone driven signal amplitudes for the N1and N1P1 components are 0.45 ± 0.21 nV/deg^2 and 0.94 ± 0.50 nV/deg^2.

Binocular Comparisons

The difference in amplitude between the L- and M-cone driven signals does not depend on which eye is recorded, as the same relation is found in the two eyes of those 23 observers from whom the mfERGs were simultaneously recorded. On average, the N1 L- to M-cone driven signal ratio of each eye in each subject deviates by 15.2 ± 11.1% from the average of both their eyes; and the N1P1 L- to M-cone driven signal ratio deviates by only 9.0 ± 9.2%. (The slightly larger deviation in the N1 signals is presumably related to the smaller signal, which is more influenced by noise.) When separately analysed by gender, the deviation between eyes is slightly smaller in the 13 males (N1 = 14.6 ± 12.0%; N1P1 = 8.3 ± 9.0%) than in the 10 females (N1 16.1 ± 9.0%; P1 10.5 ± 9.8%). A larger variance between the two eyes might be expected in females owing to local variations in the distributions of L- and M-cone photoreceptors (and hence in the cone driven signals) arising from X-chromosome inactivation (see Sharpe et al., 1999, for a review).

Full-Field and Ring Analysed L- and M-Cone Driven Waveforms

The difference in amplitude between the mean L- and M-cone driven signals is highlighted in Figure 5, which depicts the mean waveforms of the L- and M-cone driven signals of the full-field summed (lowest traces) and ring analysed (traces numbered according to the annuli depicted in Figure 1) mfERGs, averaged over all 38 subjects. Figure 5A shows the unadjusted mean L- (red curves) and M- (green curves) cone driven responses. In Figure 5B, the M-cone driven responses were normalized to the N1P1 peak of the L-cone driven one. For the central element (trace 1), the appropriate scaling factor is 1.4; for the five peripheral rings (traces 2 to 6), it is a constant value of 2.2, the same value as found for the full-field summed response (unnumbered lowest trace), which is dominated by the peripheral input. Although the scaled waveforms are very similar in shape, there are some important differences in the relative sizes of their N1 to N1P1 peaks (the two cannot be brought into perfect symmetry) and their N1 and P1 latencies differ as well.

Table 1. The N1 and N1P1 Amplitudes of the L- and M-Cone Driven mfERGs in 38 Trichromats

Subject	Eye	Gender	L-cone N1 Amplitude (nV/deg^2)	M-cone N1 Amplitude (nV/deg^2)	Ratio L/M N1 Amplitude	L-cone N1P1 Amplitude (nV/deg^2)	M-cone N1P1 Amplitude (nV/deg^2)	Ratio L/M N1P1 Amplitude
D.U.	OS	M	0.8	0.4	2.0	2.3	1.0	2.3
	OD		---	---	---	---	---	---
A.Y.	OS	F	0.3	0.5	0.6	0.8	1.3	0.6
	OD		0.6	0.5	1.2	1.4	1.3	1.1
S.H.	OS	M	0.5	0.5	1.0	1.4	1.3	1.1
	OD		---	---	---	---	---	---
M.S.	OS	M	0.9	0.8	1.1	2.5	1.0	2.5
	OD		---	---	---	---	---	---
C.W.	OS	M	1.0	0.9	1.1	3.4	2.1	1.6
	OD		1.1	0.9	1.2	3.3	2.1	1.6
N.B.	OS	F	1.3	0.3	4.3	3.4	0.5	6.8
	OD		1.0	0.3	3.3	3.6	0.6	6.0
M.B.	OS	M	1.1	0.2	5.3	3.2	0.6	5.3
	OD		1.3	0.2	6.3	3.6	0.5	7.1
K.F.	OS	F	0.9	0.5	1.8	2.1	0.6	3.5
	OD		0.7	0.4	1.8	2.3	1.0	2.3
K.G	OS	F	---	---	---	---	---	---
	OD		0.3	0.7	0.4	1.0	1.7	0.6
A.W.	OS	M	0.7	0.5	1.4	1.6	1.7	0.9
	OD		0.4	0.5	0.8	1.0	1.2	0.8
M.H.	OS	M	1.1	0.3	3.7	2.4	0.7	3.4
	OD		0.8	0.2	4.0	1.9	0.7	2.7
H.A .	OS	M	0.7	0.8	0.9	1.3	1.3	1.0
	OD		0.7	1.4	0.5	1.4	2.4	0.6
H.J.	OS	M	0.6	0.9	0.7	2.5	2.2	1.1
	OD		0.9	0.8	1.1	2.0	1.7	1.2
J.B.	OS	F	0.1	0.6	0.2	0.2	1.9	0.1
	OD		0.2	0.8	0.3	0.2	1.7	0.1
T.S.	OS	M	0.3	0.3	1.0	0.7	0.7	1.0
	OD		0.5	0.4	1.3	0.7	0.8	0.8
F.G.	OS	M	0.4	0.3	1.3	1.1	0.8	1.4
	OD		0.6	0.5	1.2	1.6	1.2	1.3
J.K.	OS	M	---	---	---	---	---	---
	OD		0.2	0.3	0.7	0.4	0.4	1.0
E.A.	OS	M	0.6	0.3	2.0	1.4	0.7	2.0
	OD		---	---	---	---	---	---
M.E.	OS	M	---	---	---	---	---	---
	OD		0.6	0.9	0.7	1.7	1.4	1.2
S.K.	OS	M	0.1	0.1	1.0	0.4	0.2	2.0
	OD		---	---	---	---	---	1.5
C.S.	OS	F	0.6	0.4	1.5	1.5	0.5	3.0
	OD		0.4	0.3	1.3	1.5	0.6	2.5
T.B.	OS	F	0.5	0.5	1.0	1.6	1.0	1.6
	OD		0.4	0.6	0.7	2.1	1.1	1.9
J.A.	OS	M	1.0	0.4	2.5	2.2	0.6	3.7

Subject	Eye	Gender	L-cone N1 Amplitude (nV/deg^2)	M-cone N1 Amplitude (nV/deg^2)	Ratio L/M N1 Amplitude	L-cone N1P1 Amplitude (nV/deg^2)	M-cone N1P1 Amplitude (nV/deg^2)	Ratio L/M N1P1 Amplitude
	OD		0.9	0.7	1.4	2.5	0.7	3.6
S.D.	OS	M	0.5	0.4	1.3	1.0	0.5	2.0
	OD		---	---	---	---	---	---
M.A.	OS	M	0.3	0.2	1.5	0.9	0.2	4.5
	OD		---	---	---	---	---	---
A.N.	OS	M	1.1	0.4	2.8	2.2	0.9	2.4
	OD		---	---	---	---	---	---
C.H.	OS	F	---	---	---	---	---	---
	OD		0.7	0.6	1.2	2.3	1.1	2.1
H.M.	OS	M	---	---	---	---	---	---
	OD		0.4	0.6	0.7	1.2	0.9	1.3
W.J.	OS	M	---	---	---	---	---	---
	OD		0.5	0.2	2.5	1.6	0.3	5.3
C.J.	OS	F	0.4	0.1	4.0	1.2	0.4	3.0
	OD		---	---	---	---	---	---
M.K.	OS	F	0.6	0.4	1.5	2.4	1.0	2.4
	OD		0.7	0.3	2.3	2.3	1.0	2.3
J.H.	OS	F	0.3	0.3	1.0	0.9	0.6	1.5
	OD		0.9	0.6	1.5	1.6	0.7	2.3
S.W.	OS	F	0.7	0.5	1.4	1.4	1.1	1.3
	OD		0.8	0.4	2.0	1.4	1.0	1.4
M.J.	OS	M	0.5	0.3	1.7	1.4	0.7	2.0
	OD		0.5	0.3	1.7	1.6	0.7	2.3
T.E.	OS	M	0.6	0.3	2.0	1.7	0.5	3.4
	OD		0.9	0.2	4.5	2.4	0.8	3.0
E.J.	OS	M	1.0	0.4	2.5	2.3	0.8	2.9
	OD		0.6	0.3	2.0	2.1	1.2	1.8
E.L.	OS	F	0.7	0.6	1.2	1.5	1.2	1.3
	OD		0.6	0.4	1.5	1.6	1.3	1.2
J.S.	OS	M	0.8	0.4	2.0	2.2	1.0	2.2
	OD		0.8	0.4	2.0	2.2	1.0	2.2
Mean ± SD			0.62 ± 0.30	0.45 ± 0.21	1.65 ± 1.12	1.65 ± 0.79	0.94 ± 0.50	2.19 ± 1.43

N1 and N1P1 amplitudes of the summed responses for 38 normal subjects. For 23 subjects, both the left (OS) and right (OD) eyes were measured, but only their left eyes (OS) were used in calculating the means.

Full-Field L- to M-Cone Driven Amplitude Ratios

In Table 1, one can compare the ratios of the L- to M-cone driven N1 (column 6) and N1P1 (column 9) component. The average L- to M-cone driven amplitude ratios for the 38 subjects is 1.65 ± 1.12 for the N1 component and 2.19 ± 1.43 for the N1P1 component. (In those 23 subjects from whom mfERGs were simultaneously recorded in both eyes, only the mfERG responses from their left eyes were used in calculating these averages.) The average value for the N1P1 component agrees perfectly with the scaling factor (2.2) calculated for the full-field summed responses (Figure5B, lowest trace). Although the L- to M-cone driven amplitudes are typically larger than unity, there is considerable variability among observers. The N1 component ratios range from 0.17 to 4.50 and the N1P1 component ratios from 0.6 to 7.10. Interestingly, the smallest values obtained for both the N1 (0.21 ± 0.06, averaged over both eyes) and N1P1 (0.11 ± 0.01, averaged over both eyes) ratios are for the female carrier of protanopia (J.B.), for whom the strength of the M-cone driven N1 (0.7 ± 0.14 nV/deg^2) and N1P1 (1.8 ± 0.14 nV/deg^2) responses is considerably greater than that for the L-cone driven N1 (0.15 ± 0.07 nV/deg^2) and N1P1 (0.2 ± 0.0 nV/deg^2) responses.

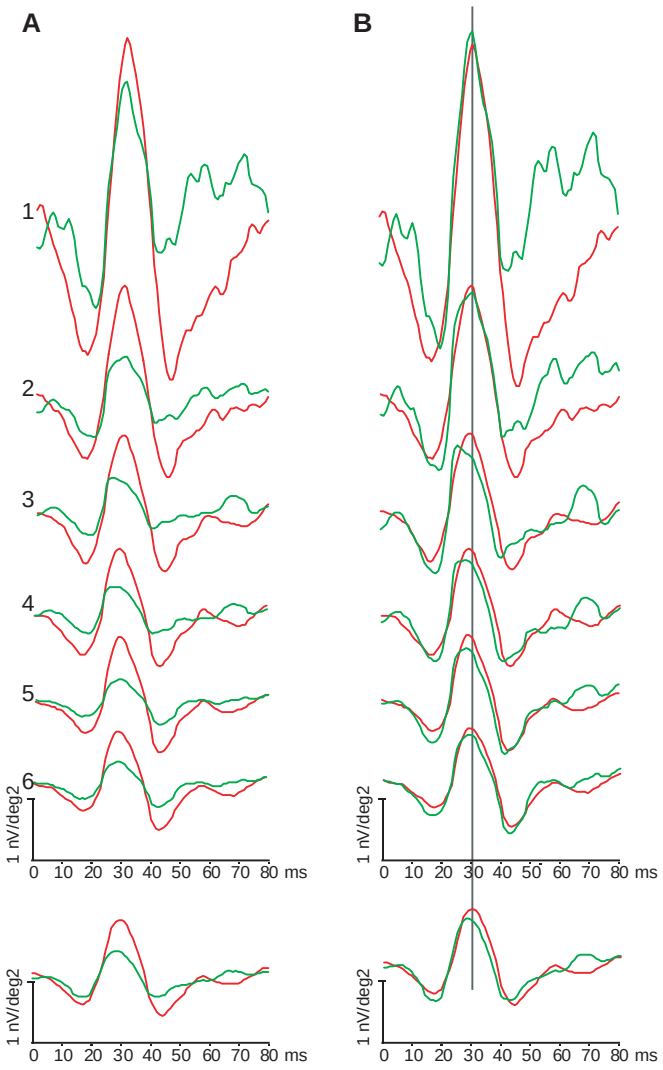

Figure 5. mfERG responses for L- (red curves) and M- (green curves) cone driven signals averaged for 38 normal subjects. For 23 subjects, both the left (OS) and right (OD) eyes were measured, but only their left eyes (OS) were used in the average. The lowest pair of traces is for the full-field summed response; see Figure 1 for the numbered traces for the ring analysed responses. A. The unadjusted mean L- and M-cone driven amplitudes; B. The M-cone driven amplitude normalized to the N1P1 peak of the L-cone driven one.

L- and M-Cone Driven Amplitudes and Retinal Eccentricity

Figure 6A plots the change in mean L- (red curves) and M- (green curves) cone driven N1 and N1P1 amplitudes as a function of retinal eccentricity (the values were obtained after summing the responses for all subjects within the concentric rings depicted in Figure 1). For both the N1 and N1P1 components, the amplitudes are largest for the central ring (5° dia.) and typically fall off sharply with eccentricity up to 10° in the periphery and remain almost constant thereafter. Figure 6B shows the L- to M-cone driven amplitude ratios for N1 and N1P1, determined from the same data, as a function of retinal eccentricity. They are consistent with the scaling factors derived in Figure 5B by normalizing the M-cone driven N1P1 peaks to the L-cone driven ones. Mean values and standard deviations can be calculated by averaging the individual data analysed according to rings. For the central fovea (5° dia.), the mean ratios are 1.3 ± 0.8 (N1) and 1.4 ± 0.6 (N1P1); whereas, for the annular ring centred at 40° in the periphery, they are 1.7 ± 1.2 (N1) and 2.3 ± 2.0 (N1P1).

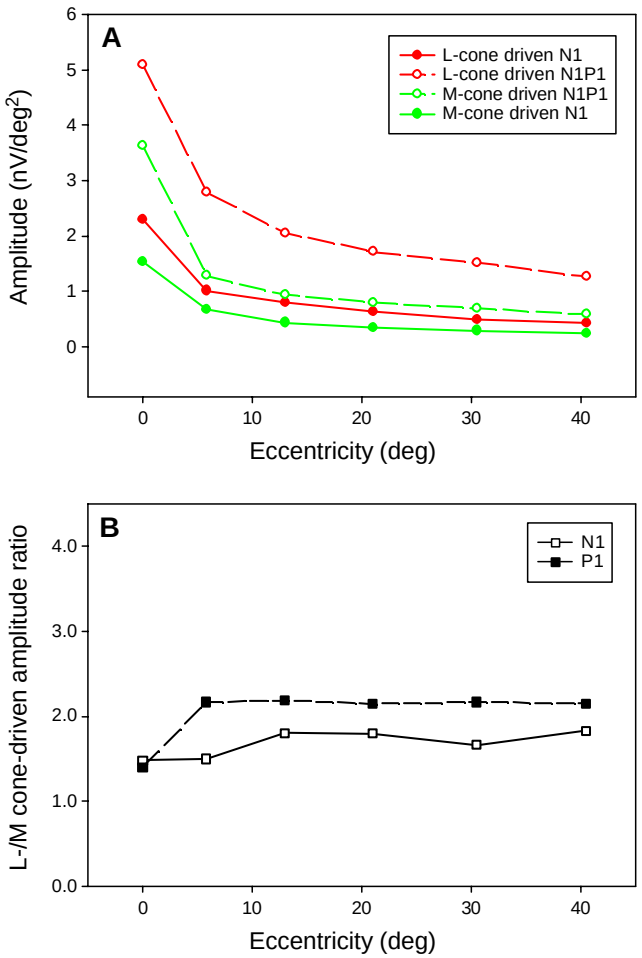

Figure 6. A. The variation in the amplitude of the N1 (filled circles) and N1P1 (open circles) components of the L- (red symbols) and M- (green symbols) cone driven mfERGs as a function of retinal eccentricity. The individual hexagonal response traces have been summed according to the six concentric rings depicted in Figure 1. B. The L- to M-cone driven mfERG ratios, derived from the summed responses, as a function of retinal eccentricity for both the N1 (open symbols) and N1P1 (filled symbols) components.

Table 2. The N1 and P1 Latencies of the L- and M-Cone Driven mfERGs in 38 Trichromats

Subject	Eye	Gender	L-cone N1 Latencies (ms)	M-cone N1 Latencies (ms)	Difference L-M N1 Latency	L-cone P1 Latencies (ms)	M-cone P1 Latencies (ms)	Difference L-M P1 Latency
D.U.	OS	M	16.9	16.9	0.0	30.9	30.9	0.0
	OD		---	---	---	---	---	---
A.Y.	OS	F	18.3	16.6	1.7	29.1	28.2	0.9
	OD		15.8	16.6	-0.8	29.1	26.6	2.5
S.H.	OS	M	15.9	15.9	0.0	27.2	25.3	1.9
	OD		---	---	---	---	---	---
M.S.	OS	M	14.0	16.9	-2.9	28.1	27.0	1.1
	OD		---	---	---	---	---	---
C.W.	OS	M	16.6	14.1	2.5	27.5	26.6	0.9
	OD		15.0	15.0	0.0	28.3	25.8	2.5
N.B.	OS	F	16.6	13.3	3.3	28.3	24.1	4.2
	OD		15.0	17.5	-2.5	27.5	27.0	0.5
M.B.	OS	M	17.5	19.1	-1.6	28.3	28.3	0.0
	OD		16.6	18.3	-1.7	28.3	29.1	-0.8
K.F.	OS	F	18.3	14.1	4.2	27.4	26.6	0.8
	OD		13.3	15.8	-2.5	26.6	24.9	1.7
K.G.	OS	F	---	---	---	---	---	---
	OD		17.4	16.6	0.8	31.5	29.1	2.4
A.W.	OS	M	15.8	18.3	-2.5	27.4	28.2	-0.8
	OD		16.6	18.3	-1.7	29.9	29.9	0.0
M.H.	OS	M	16.6	13.3	3.3	28.2	33.2	-5.0
	OD		15.8	19.1	-3.3	29.9	30.7	-0.8
H.A.	OS	M	15.0	16.9	-1.9	31.8	30.0	1.8
	OD		15.0	15.9	-0.9	30	26.2	3.8
H.J.	OS	M	19.7	15.9	3.8	30	29.0	1.0
	OD		19.7	15.9	3.8	30	30.0	0.0
J.B.	OS	F	16.9	15.1	1.8	28.1	27.2	0.9
	OD		13.1	17.8	-4.7	25.3	28.1	-2.8
T.S.	OS	M	15.9	14.0	1.9	30.9	30.0	0.9
	OD		17.8	15.0	2.8	32.8	30.9	1.9
F.G.	OS	M	16.9	15.9	1.0	30.9	29.0	1.9
	OD		16.9	15.9.	1.0	29	29.0	0.0
J.K.	OS	M	---	---	---	---	---	---
	OD		16.9	14.0	2.9	27.2	24.3	2.9
E.A.	OS	M	17.8	16.9	0.9	34.6	34.0	0.6
	OD		---	---	---	---	---	---
M.E.	OS	M	---	---	---	---	---	---
	OD		15.9	15.9	0.0	31.8	30.9	0.9
S.K.	OS	M	14.1	16.6	-2.5	31.6	28.2	3.4
	OD		---	---	---	---	---	---
C.S.	OS	F	16.6	15.8	0.8	28.2	29.9	-1.7
	OD		16.6	15.8	0.8	28.2	28.2	0.0
T.B.	OS	F	14.9	14.9	0.0	26.6	28.2	-1.6
	OD		19.1	17.4	1.7	28.2	29.9	-1.7
J.A.	OS	M	16.6	14.9	1.7	28.2	30.7	-2.5

Subject	Eye	Gender	L-cone N1 Latencies (ms)	M-cone N1 Latencies (ms)	Difference L-M N1 Latency	L-cone P1 Latencies (ms)	M-cone P1 Latencies (ms)	Difference L-M P1 Latency
	OD		16.6	15.0	1.6	29.1	27	2.1
S.D.	OS	M	14.9	16.6	-1.7	28.2	30.7	-2.5
	OD		---	---	---	---	---	---
M.A.	OS	M	16.6	14.1	2.5	29.1	24.9	4.2
	OD		---	---	---	---	---	---
A.N.	OS	M	14.9	15.8	-0.9	26.6	24.9	1.7
	OD		14.9	15.8	-0.9	27.4	27.4	0.0
C.H.	OS	F	---	---	---	---	---	---
	OD		16.6	14.9	1.7	26.6	26.4	0.2
H.M.	OS	M	---	---	---	---	---	---
	OD		15.8	13.3	2.5	30.7	24.1	6.6
W.J.	OS	M	---	---	---	---	---	---
	OD		16.6	14.9	1.7	29.9	24.1	5.8
C.J.	OS	F	17.4	14.1	3.3	28.7	31.6	-2.9
	OD		---	---	---	---	---	---
M.K.	OS	F	14.1	16.6	-2.5	27.4	29.1	-1.7
	OD		14.1	15.8	-1.7	27.4	29.1	-1.7
J.H.	OS	F	14.9	14.1	0.8	29.1	23.5	5.6
	OD		16.6	15.8	0.8	27.4	24.1	3.3
S.W.	OS	F	14.9	17.4	-2.5	27.9	27.4	0.5
	OD		15.8	17.4	-1.6	30.7	29.1	1.6
M.J.	OS	M	15.8	19.1	-3.3	29.5	29.0	0.5
	OD		14.1	14.9	-0.8	29.1	31.6	-2.5
T.E.	OS	M	15.8	14.9	0.9	27.4	24.9	2.5
	OD		14.9	14.1	0.8	27.4	24.1	3.3
E.J.	OS	M	17.4	14.0	3.4	31.6	31.6	0.0
	OD		17.4	14.9	2.5	29.9	28.2	1.7
E.L.	OS	F	16.6	16.6	0.0	29.9	26.6	3.3
	OD		13.3	15.8	-2.5	28.2	26.6	1.6
J.S.	OS	M	14.9	11.6	3.3	26.6	26.6	0.0
	OD		15.8	14.9	0.9	27.4	29.1	-1.7
Mean ±SD			16.2±1.3	15.6±1.7	0.6±12.1	29.0±1.9	28.0±2.6	1.0±2.4

N1 and P1 latencies of the summed responses for 38 normal subjects. For 23 subjects, both the left (OS) and right (OD) eyes were measured, but only their left eyes (OS) were used in calculating the means.

L- and M-Cone Driven Latencies

Figure 5 (lower traces) clearly illustrates the difference in latency between the average L- and M-cone driven full field mfERG signals. The difference for both the N1 and P1 components is quantified for each subject in Table 2 (see columns 6 and 9, respectively).

The mean latency of the N1 component of the M-cone driven signal (15.6 ± 1.7 ms) is slightly advanced relative to that of the L-cone driven signal (16.2 ± 1.3 ms). (In those 23 subjects from whom mfERGs were simultaneously recorded in both eyes, only the mfERG responses from their left eyes were used in calculating these averages.) However, the difference is not statistically significant; and there is considerable variability among subjects in the latency difference. In fact, for 12 of the 38 subjects, the L-cone driven N1 latency is actually shorter than the M-cone driven one. In contrast, the mean latency of the P1 component of the M-cone driven signal (28.0 ± 2.6 ms) is significantly advanced (paired *t* test: $p = .015$, N = 38) relative to that of the L-cone driven signal (29.0 ± 1.9 ms). For only 8 of the subjects is the L-cone driven P1 latency shorter than the M-cone driven one.

L- and M- Cone Driven Latency and Retinal Eccentricity

Figure 7 plots the mean latencies of the L- and M-cone driven mfERG signals analysed within concentric rings (see Figure 1). For the N1 component (filled symbols, N = 34; for 4 of the subjects [J.B., M.A., W.J., and C.J.], the signals were too noisy for a reliable ring analysis), the latencies of the M- and L-cone driven signals are very similar and do not vary significantly with retinal eccentricity. In contrast, for the P1 component (open symbols, N = 37; for subject S.H., the signals were too noisy for a ring analysis), both the M- and L-cone driven signals show a significant decrease in latency with eccentricity. Except for the most central ring (5° dia.), the P1 latencies of the M- and L-cone driven signals also differ significantly. For all other rings, the M- cone driven latency is significantly advanced relative to the L-cone driven signal. These changes are also obvious when inspecting the ring analysis provided in Figure 5B (traces 1 to 6).

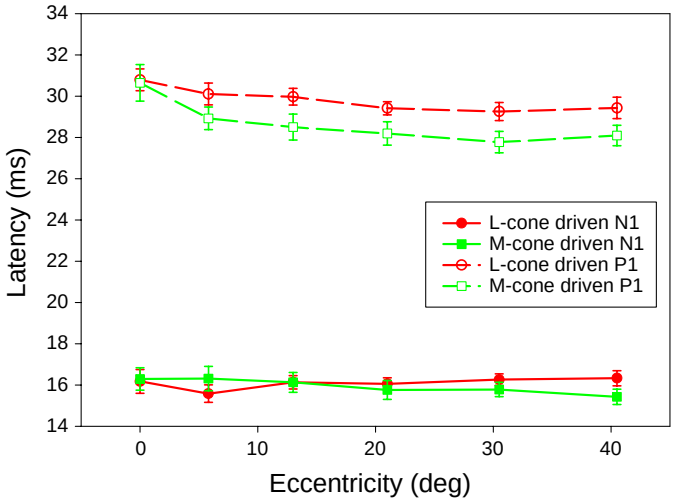

Figure 7. The variation in the latency of the N1 (filled symbols) and P1 (open symbols) components of the L- (red symbols) and M- (green symbols) cone driven mfERGs as a function of retinal eccentricity. The individual hexagonal response traces have been summed according to the six concentric rings depicted in Figure 1. Means and standard deviations are shown for 34 observers for the N1 (S.H., M.A., W.J., and C.J. were excluded) and 37 observers for the P1 (S.H . was excluded).

Correlation with Heterochromatic Flicker Photometry

Large differences between the strengths of inferred M- and L-cone isolated responses have been reported in previous psychophysical (De Vries, 1946, 1948; Cicerone & Nerger, 1989; Vimal et al., 1989; Pokorny et al., 1991; Wesner et al., 1991; Kremers et al., 2000) and ERG flicker studies (Carroll et al., 2000; Kremers et al., 2000). The results from different procedures measured in the same observers can correlate highly with one another (see Kremers et al., 2000) and have been used to draw inferences about the relative L- to M-cone numbers in the retinal mosaic. To determine if our L- to M-cone driven mfERG amplitude ratios also correlate with such measures, we derived estimates of L- to M-cone ratios from full-spectrum (400 to 690 nm) heterochromatic flicker photometric (HFP) thresholds measured in 16 of our 38 observers. The HFP measurements were made for a 2° dia., 25 Hz flickering target presented in counterphase with a reference light (560 nm) on a xenon arc background (3 log photopic td, color temperature 6500 K) 16° dia. (for a detailed description of the procedure, see Kremers, Usui, Scholl, & Sharpe, 1999). Therefore, in making comparisons with the HFP data, we restricted the mfERG data to the inner part of the visual field to minimize regional variations influencing the results. The comparisons are shown in Figure 8 for both the N1 and N1P1 components for the summed inner 20° mfERG response (i.e., grouped over the four inner rings). The best correlation, r^2=0.83, is obtained between the 2° HFP data and the 20° N1P1 data (slope = 0.69). In contrast, the correlation between the 2° HFP data and the 20° N1 data is r^2=0.68 (slope = 0.52); and, the correlation between the 2° HFP data and the inner 5° mfERG N1P1 data is only r^2=0.51 (slope = 0.30). As the HFP data have a symmetrical distribution on a log scale (see references cited in Table 1b

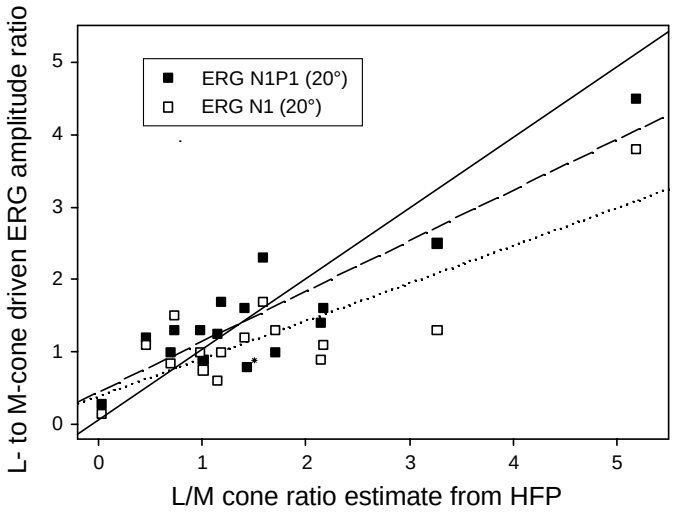

Figure 8. L-cone to M-cone driven amplitude ratios derived from the N1 (open symbols) and N1P1 (filled symbols) amplitudes of isolated cone driven mfERG responses plotted against estimates derived from linear fits to (2°) HFP thresholds in 16 normal observers. The comparisons with the HFP are shown for hexagonal responses summed within the inner 20° of the visual field for the N1 (slope = 0.52; r^2=0.68; large dashed lines) and N1P1 (slope = 0.69; r^2=0.83; small dashed lines) components. The solid line (slope = 1.0) indicates a perfect correlation and the locus of equal values. For one subject (marked with a small star), L- to M-cone driven ratios derived from the N1 and N1P1 amplitudes are the same. See text for other details.

of Pokorny et al., 1991), correlations were also obtained between the HFP data and the log L- to M-cone driven amplitude ratio. These values were similar to those above, r^2=0.72 for the 2° HFP and the 20° N1P1 data, r^2=0.70 for the 2° HFP and the 20° N1 data, and r^2=0.65 for the 2° HFP and the inner 5° mfERG N1P1 data.

Discussion

Inferring L- to M-Cone Ratios From mfERG Amplitudes

Given that the mfERG provides a topographical representation of these cone driven signals, we wanted to determine if those signals could be used to draw inferences about L- to M-cone ratios in the retina. Admittedly, in doing so, we must be cautious because the interpretation of the elicited mfERG waveforms is complicated. The only previous study concerned with L- and M-cone isolating stimuli and the mfERG (Klistorner, Crewther, & Crewther, 1998) varied the contrast of the color hexagonal elements so as to pass through the isoluminance condition (i.e., so that there was apparently only red-green opponent channel and no luminance contrast information available). Their silent substitution condition for the L cones was near a contrast ratio of 0.49 or about 35%, whereas their silent substitution for the M cones was near a green/red ratio of 1.39 or about 16%. Thus, they could not directly compare L- and M-cone driven response amplitudes, and their data cannot be used to derive L- to M-cone driven ratios.

To relate the relative amplitudes of L- and M-cone driven mfERGs to L- and M-cone ratios in the retinal mosaic, it is necessary to start with stimuli that provide equivalent L- or M-cone inputs to the rest of the visual system. For this reason, we chose the mean luminances of our L- (19.2 cd/m^2) and M- (33.8 cd/m^2) cone isolating stimuli to obtain equal quantal catches, ensuring that both cone classes were stimulated at the same adapting level. Additionally, it is necessary to demonstrate that the four following conditions are satisfied: (1) that the amplitude versus intensity relations are similar for both the L- and M-cone isolating stimuli; (2) that the relations between the L- and M-cone driven signals are constant at different contrast levels; (3) that the response waveforms to the L- and M-cone isolating stimuli are similar; and (4) that the mfERG the L- to M-cone estimates correlate with estimates obtained with other techniques.

Figures 3 and 4 demonstrate that the first two criteria hold to a first approximation: namely, that the amplitude versus intensity functions of the L- and M-cone driven signals are similar and the two signals are linear with contrast for the values falling within the critical measuring range. Further, the comparisons in Figure 8 indicate that the fourth criterion is also roughly fulfilled, insofar as the 20° mfERG (N1P1) and 2° HFP estimates obtained from the same group of observers correlate with one another. And, the average L- to M-cone driven amplitude ratio of 2.19 ± 1.43 for the N1P1 component correlates very well with the values found by many other psychophysical and electroretinographic studies estimating the relative numbers of L- and M- cones (cf., Kremers et al., 1999). In addition, the M-cone dominated estimates, obtained from the mfERG recordings in the carrier for protanopia, accord with other reports suggesting a strong dominance of the M cones in such carriers (Crone, 1959; Miyahara, Pokorny, Smith, Baron, & Baron, 1998).

Figure 5 suggests that the third criterion, uniformity of the L- and M-cone driven waveforms, also roughly holds not only for the full field but also for the ring analyses (granted the absolute amplitudes of the mean L- and M-cone driven signals differ [which was to be expected] and the relative sizes of their N1 to N1P1 peaks and their N1 and P1 latencies differ as well). This results in the magnitude of the L- to M-cone driven amplitude ratio being greater for the N1P1 component than for the N1 component. However, the general similarity between them suggests that our simplifying assumptions are reasonable at least to a first approximation.

L- to M-Cone Ratios and Retinal Eccentricity

Given the differences in waveform between the L- and M-cone driven signals, in the peripheral retina, only tentative conclusions can be drawn about the change in L- to M-cone driven amplitude ratio with eccentricity. On the one hand, the difference between the central (5° dia.) and peripheral (>10° eccentricity) L/M-cone amplitude ratios for both N1 and N1P1 accords with the results of preliminary molecular biological studies in which the L- to M-cone pigment mRNA ratio increased substantially between central and peripheral patches (Hagstrom et al., 1997, 1998). But, the increase in the mfERG L- to M-cone driven amplitude ratios may only be apparent. It seems unlikely that most individuals have a more similar L- to M-cone ratio in the very central fovea than in the parafoveal and more peripheral regions. Indeed, this interpretation is supported by direct visualization of the foveal cone mosaic with adaptive optics. In their study, Roorda and Williams (1999) found very different L- to M-cone ratios (about 1.1:1 and 3.8:1) in two color normal observers measured in small (<30 min of arc dia.) patches at 1° eccentricity. This is the sort of variability found among observers in the peripheral but not in the central L/M-cone ratio mfERG estimates.

Thus, we would argue that the differences in L- to M-cone ratios between the central and peripheral mfERG responses may reflect other factors. One of these may be that the center element of the mfERG is more noise limited than the peripheral elements. However, the most important factor could be a change in gain between the

receptors and bipolars that depends upon eccentricity. The photopic mfERG, like the photopic full-field ERG, is dominated by the bipolar response (e.g., Horiguchi et al., 1998; Hare et al., 2001; Hood et al., 2002a). As the size and mix of the bipolar cells change with eccentricity, the relative gain of the L- and M-cone signal may be altered. There are various ways the gain change argument can be developed, given a typical retinal cone mosaic in which the L cones predominate (say a 2L:1M ratio arrangement). Consider first that the midget bipolars have only a single cone in the center (i.e., either a L- or M-cone), but that the extent of the midget bipolar surrounds is spatially constrained so that the number of cone inputs depends upon cell type. In that case, the L- to M-cone driven ratio in the central fovea may be underestimated because midget cone bipolar surrounds will reflect the local ratio if they sample cones selectively, either all M- or all L-cones (i.e., there will be more L cones opposing an M cone ON center midget bipolar cell than M cones opposing an L cone ON center midget bipolar). Even though they may have twice as many L-cone center ON-bipolar cells, their responses will be smaller than those of the M-cone center ON bipolar cells, because their surrounds will have twice the input compared with the M center ON-bipolar cells. On the other hand, if the input to the surround is selective but not spatially constrained so that it always consists of the same number of cones (say 6) but of the other cone type (i.e., either all M- or all L-cones), then the response of an L-cone center midget cell will be inhibited by the input of 6 M cones and the response of the M-center midget bipolar cell will be inhibited by 6 L cones. The influence on sensitivity should be roughly the same. But, if the input to the surround is not spatially constrained and is random and nonselective (which seems the most likely possibility), then the response of both the L-cone center and M-cone center midget bipolar cells would be inhibited by twice as many L cones as M cones, and the L-cone center would have a smaller response due to greater "self-inhibition." Thus, the net effect would be a smaller L- to M-cone driven amplitude ratio in the central fovea than in the periphery.

Latency Differences Between the L- and M-Cone Driven Signals

Our results reveal a 1.0-ms difference in the latency of the P1 component between the L- and M-cone driven signals with the M-cone driven response being significantly advanced. The difference between the L- and M-cone driven N1 latencies is smaller (0.6 ms) and is not significant. The P1 results accord with previous results reported by Weithmore and Bowmaker (1995) and by Kremers et al. (1999), who found a phase difference equal to circa 1.4 ms between the L- and M-cone driven Ganzfeld flicker ERGs.

It is important not to interpret these latency differences as directly reflecting differences in the response properties of the L- and M-cones per se. This is for several reasons. First, the mfERG is a complex waveform. If, for example, the positive component driving P1 (driven in part by the ON-bipolars [the PII component of Granit]) is slightly faster for the M-cone isolation mode than for the L-cone isolation mode, then the implicit time of N1, which is really the algebraic sum of the ON-bipolar cell response and a negative potential(s), will be shorter for the M-cone than for the L-cone driven signals. Second, the differences in N1 and P1 latency between the L- and M-cone driven mfERG signals are not found in the central fovea (see Figure 7), where the amplitude evidence suggests that post-receptoral components distort the waveforms the least (see Figure 5). Third, the differences in latency between the L- and M-cone driven signals do not depend on the relative differences in the size of the L- and M-cone driven amplitudes. Larger amplitude signals are not associated with longer latencies (i.e., the N1 and P1 latency differences between the L- and M-cone driven signals depend on neither the L- to M-cone driven N1 nor on the L- to M-cone driven N1P1 amplitude ratio).

Conclusions

The 20° L- to M-cone driven N1P1 amplitude ratios correlate with the psychophysically measured 2° HFP data, and estimates obtained in each observer for the N1 and N1P1 components correlate highly with one another (r^2 = 0.68 and 0.83, respectively). Therefore, we can conclude that the L- to M-cone ratio in the foveal center as well as periphery differs with individuals. Although L- to M-cone driven amplitude ratios are larger for N1P1 versus N1 and larger for >5° versus < 5°, these ratios vary among individuals and are highly correlated within an individual. The changes with retinal eccentricity probably do not merely reflect noise limitations (the central mfERG responses are more noise limited than the peripheral ones) nor an abrupt change in the L- to M-cone ratio of the central as contrasted with the peripheral retina. Rather, they emphasize the need to look more closely at differences between central and peripheral retinal processing. The opportunity to examine the central responses, in terms of different pathway contributions, is afforded by the mfVEP, which overcomes the signal to noise limits imposed on small central visual fields in the mfERG. It exploits the cortical magnification of the foveal response to obtain estimates of visual processing within the inner 1.2° (radius) of visual field, where the parvocellular pathways dominate. We have recently recorded mfVEP responses to L- and M-cone isolating stimuli (Hood et al., 2002b). The central mfVEP responses are similar in amplitude and waveform for observers, but the peripheral responses differ in amplitude and waveform with the L-cone

modulation producing larger responses. Taken together, the mfVEP and mfERG results suggest that there is a change in gain in the PC pathway before the mfVEP is generated in area 17 and that some of this gain change may be occurring before the midget bipolar cell response in the outer plexiform layer.

Acknowledgments

This work was supported by a Lilly-und-Hermann-Schilling-Stiftung (Essen, Germany) Professorship and by grants SFB 430 (TP A6) and Sh23/5-2 awarded by the Deutsche Forschungsgemeinschaft (Bonn-Bad Godesberg, Germany) to L.T.S. and by grants from the Landesswerpunkprogramm Baden-Würtemberg and the fortüne-Programme (780-0-0, Universitäts-Klinikum Tübingen) awarded to H.J. and L.T.S. The authors would like to thank Emanuela de Luca for help with the graphics.

Commercial Relationships: None.

References

Carroll, J., McMahon, C., Neitz, M., & Neitz, J. (2000). Flicker-photometric electroretinogram estimates of L:M cone photoreceptor ratio in men with photopigment spectra derived from genetics. *Journal of the Optical Society of America A, 17*, 499-509. [PubMed]

Cicerone, C. M., & Nerger, J. L. (1989). The relative numbers of long-wavelength-sensitive to middle-wavelength-sensitive cones in the human fovea centralis. *Vision Research, 26*, 115-128. [PubMed]

Crone, R. A. (1959). Spectral sensitivity in color-defective subjects and heterozygous carriers. *American Journal of Ophthalmology, 48*, 231-238.

De Vries, H. L. (1946). Luminosity curve of trichromats. *Nature, 15*, 736-737.

De Vries, H. L. (1948). The heredity of the relative numbers of red and green receptors in the human eye. *Genetica, 24*, 199-212.

Hagstrom, S. A., Neitz, J., & Neitz, M. (1997). Ratio of M/L pigment gene expression decreases with retinal eccentricity. In C. R. Cavonius (Ed.), *Colour vision deficiencies XIII* (pp. 59-65). Dordrecht, The Netherlands: Kluwer.

Hagstrom, S. A., Neitz, J., & Neitz, M. (1998). Variation in cone populations for red-green color vision examined by analysis of mRNA. *NeuroReport, 9*, 1963-1967. [PubMed]

Hare, W. A., Ton, H., Ruiz, G., Feldmann, B., Wijono, M., & WoldeMussie, E. (2001). Characterization of retinal injury using ERG measures obtained with both conventional and multifocal methods in chronic ocular hypertensive primates. *Investigative Ophthalmology & Visual Science, 42*, 127-136. [PubMed]

Hood, D. C. (2000). Assessing retinal function with the multifocal technique. *Progress in Retinal and Eye Research, 19*, 607-646. [PubMed]

Hood, D. C., Frishman, L. J., Saszik, S., & Viswanathan, S. (2002a). Retinal origins of the primate multifocal ERG: Implications for the human response. *Investigative Ophthalmology & Visual Science, 43*, 1673-1685. [PubMed]

Hood, D. C., Seiple, W., Holopigian, K., & Greenstein, V. (1997). A comparison of the components of the multi-focal and full-field ERGs. *Visual Neuroscience, 314*, 533-544. [PubMed]

Hood, D. C., Yu, A. L., Zhang, X., Albrecht, J., Jägle, H., & Sharpe, L. T. (2002b). The multifocal visual evoked potential and cone-isolating stimuli: Implications for L- to M-cone ratios and normalization. *Journal of Vision*, 2(2), 178-189, http://journalofvision.org/2/2/4/, DOI 10.1167/2.2.4. [Link]

Horiguchi, M., Suzuki, S., Kondo, M., Tanikawa, A., & Miyake, Y. (1998). Effect of glutamate analogues and inhibitory neurotransmitters on the electroretinograms elicited by random sequence stimuli in rabbits. *Investigative Ophthalmology & Visual Science, 39*, 2171-2176. [PubMed]

Klistorner, A., Crewther, D. P., & Crewther, S. G. (1998). Temporal analysis of the topographic ERG: Chromatic versus achromatic stimulation. *Vision Research, 38*, 1047-1062. [PubMed]

Kremers, J., Usui, T., Scholl, H. P., & Sharpe, L. T. (1999). Cone signal contributions to electroretinograms in dichromats and trichromats. *Investigative Ophthalmology & Visual Science, 40*, 920-930. [PubMed]

Kremers, J., Scholl, H. P. N., Knau, H., Berendschot, T. T. T. M., Usui, T., & Sharpe, L. T. (2000). L/M cone ratios in human trichromats assessed by psychophysics, electroretinography, and retinal densitometry. *Journal of the Optical Society of America A, 17*, 517-526. [PubMed]

Miyahara, E., Pokorny, J., Smith, V. C., Baron, R., & Baron, E. (1998). Color vision in two observers with highly biased LWS/MWS cone ratios. *Vision Research, 38*, 601-612. [PubMed]

Nathans, J., Thomas, D., & Hogness, D. S. (1986). Molecular genetics of human color vision: The genes encoding blue, green, and red pigments. *Science*, *232*, 193-232. [PubMed]

Pokorny, J., Smith, V. C., & Wesner, M. F. (1991). Variability in cone populations and implications. In A.Valberg & B. B. Lee (Eds.), *From pigments to perception: Advances in understanding visual processes* (pp. 1-9). New York: Plenum Press.

Pugh, E. N. (1988). Vision: Physics and retinal physiology. In R. C. Atkinson (Ed.), *Stevens handbook of experimental psychology* (pp. 75-163). New York: Wiley.

Roorda, A., & Williams, D. R. (1999). The arrangement of the three cone classes in the human eye. *Nature, 397*, 520-522. [PubMed]

Sharpe, L. T., Stockman, A., Jägle, H., Knau, H., & Nathans, J. (1999). L-, M- and L-M-hybrid cone photopigments in man: Deriving λ_{max} from flicker photometric spectral sensitivities. *Vision Research*, *39*, 3513-3525. [PubMed]

Sieving, P. A., Murayama, K., & Naarendorp, F. (1994). Push-pull model of the primate photopic electroretinogram: A role for hyperpolarizing neurons in shaping the b-wave. *Visual Neuroscience, 11*, 519-532. [PubMed]

Sutter, E. E. (1991). The fast m-transform: A fast computation of cross-correlations with binary m-sequences. *Society for Industrial and Applied Mathematics*, *2*, 686-694.

Sutter, E. E., & Tran, D. (1992). The field topography of ERG components in man. I. The photopic luminance response. *Vision Research*, *32*, 433-446. [PubMed]

Stockman, A., & Sharpe, L. T. (1998). Human cone spectral sensitivities: A progress report. *Vision Research*, *38*, 3193-3206. [PubMed]

Stockman, A., & Sharpe, L. T. (1999). Cone spectral sensitivities and color matching. In K. Gegenfurtner & L. T. Sharpe (Eds.), *Color vision: From genes to perception* (pp. 53-88). Cambridge: Cambridge University Press.

Stockman, A., & Sharpe, L. T. (2000). The spectral sensitivities of the middle- and long-wavelength sensitive cones derived from measurements in observers of known genotype. *Vision Research*, *40*, 1711-1737. [PubMed]

Vimal, R. L. P., Pokorny, J., Smith, V. C., & Shevell, S. K. (1989). Foveal cone thresholds. *Vision Research*, *29*, 61-78. [PubMed]

Weithmore, A. V., & Bowmaker, J. K. (1995). Short communication: Differences in the temporal properties of human longwave- and middlewave-sensitive cones. *European Journal of Neuroscience*, *7*, 1420-1423. [PubMed]

Wesner, M., Pokorny, J., Shevell, S. K., & Smith, V. C. (1991). Foveal cone detection statistics in color-normals and dichromats. *Vision Research*, *31*, 1021-1037. [PubMed]

Wyszecki, G., & Stiles, W. S. (1982). *Color science: Concepts and methods, quantitative data und formulae* (2nd ed.). New York: Wiley.